Interdisciplinary Research for a Geothermal Carbonate Reservoir

Hermann Buness[1], Hartwig von Hartmann[1], Jennifer Ziesch[1,2], Britta Wawerzinek[1,3], Ernesto Meneses Rioseco[1], Ruediger Thomas[1]

[1] Leibniz Institute for Applied Geosciences, Stilleweg 2, 30655 Hannover

[2] now at State Authority for Mining, Energy and Geology (LBEG), Stilleweg 2, 30655 Hannover

[3] now at Helmholz center Potsdam (GFZ), Telegrafenberg, D-14473 Potsdam

hermann.buness@leibniz-liag.de

Keywords: carbonate reservoir, 3D-seismic cube, seismic classification, seismic sequence stratigraphy, retro-deformation, s-waves, dolomitization, TH-modelling, multi-well pattern

ABSTRACT

The Upper Jurassic carbonate platform in the Bavarian Molasse Basin will be extensively used to provide the district heating system of Munich with geothermal energy. We take an interdisciplinary approach to examine a large 3D-seismic volume, without well information. The project GeoParaMoL is part of the GRAME project coordinated by the Stadtwerke München (SMW).

Seismic facies analysis reveals the distribution of different carbonate rocks by analyzing seismic reflection patterns. We divided the 600 m thick platform vertically; in each layer, a classification based on seismic attributes was computed. On top of this, we applied seismic sequence analysis along sections through the platform to interpret the classifications.

Furthermore, we use multicomponent recordings to conduct a converted wave processing, giving the relationship of P- to S-wave velocity ratio (v_p/v_s) for a part of the reservoir. Results show an unexpected high v_p/v_s for the Molasse units, which has consequences for hypocentre determination of induced seismicity. Inside the reservoir, regions with low v_p/v_s ratio correlate with patterns derived from facies analysis. High v_p and v_s values correlate with low v_p/v_s and indicate dolomitized carbonates.

Retro-deformation enables the prediction of sub-seismic faults that are invisible for seismic interpretation. A surprising result regarding the most prominent fault shows the largest strain occurred not near the fault, but approximately 500 m to 1000 m south of it. We found significant strain variations along the fault strike.

Combination of these methods yields a more complete picture of the geothermal reservoir. A reservoir model of the GRAME region enables a coupled thermal-hydraulic (TH) simulation and volumetric analysis. To achieve this, we generated numerically stable 3D finite element grids to handle topologically complex structures and strong hydraulic gradients at sharp lateral and vertical permeability contrasts.

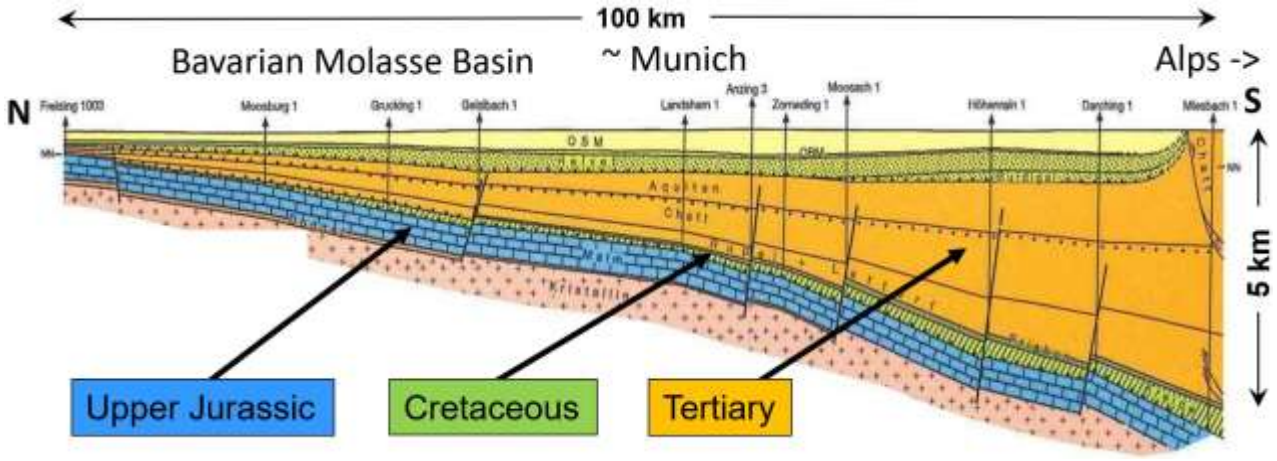

Figure 1: Simplified sketch of the geology of the Bavarian Molasse Basin (Fritzer et al. 2004). The geothermal reservoir is inside the Upper Jurassic (Malm) units, overlain by southwards increasing thick Molasse units. Beneath Munich, they reach a thickness of 2 – 3 km. Cretaceous layers thin out towards the NW in the survey area.

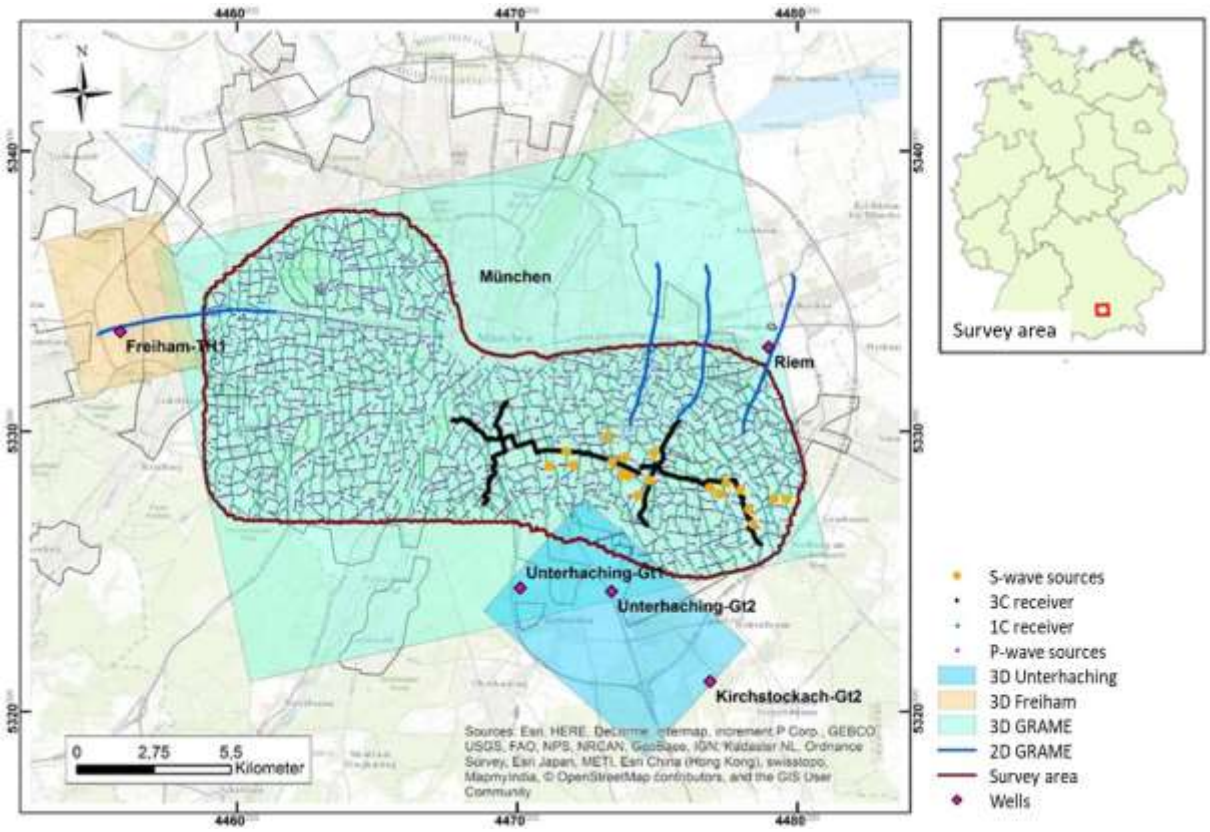

Figure 2: 3D-seismic survey covering the southern and western part of Munich, adjacent 2D- and 3D- surveys and surrounding geothermal wells.

1. INTRODUCTION

The Upper Jurassic (Malm) carbonate platform in the Bavarian Molasse Basin (Fig. 1), is the most important hydrogeothermal reservoir in Germany. 27 geothermal facilities are already in operation, however the potential has not yet been completely exploited. In the southern part of Munich, the 'Stadtwerke München' envisage a 100% supply of sustainable heat energy by the year 2040; geothermal heat shall contribute by an area-wide pattern of geothermal facilities comprising of up to 50 new boreholes (Project GRAME, Hecht and Pletl 2015).

Geothermal boreholes in the Malm have shown, that despite many successful projects, also some failures occurred (e.g. Geretsried, Mauerstetten), emphasizing the need for comprehensive characterization of potential geothermal reservoirs. This is the intention of the GeoParaMoL project (Buness et al. 2016) of the Leibniz Institute for Applied Geophysics (LIAG), that uses (1) seismic attribute analysis, (2) S-wave experiments, (3) structural analysis, including retro-deformation, and (4) thermal-hydraulic modelling to achieve this aim.

As a database for the project, a 3D-seismic survey was acquired that covers 170 km² of the southern part of Munich (Fig. 2). The survey was carried out 2016/17; the processing included pre-stack depth migration. This yielded the best image and was subsequently used for interpretation. It should be mentioned that no well existed during the time of the project that penetrates the Malm unit in the survey area. 2D profiles were shot to connect boreholes in the surrounding area for depthing. Shear wave measurements were also conducted during the regular 3D-seismic survey (s. Fig. 2). In a passive experiment, the survey was additionally recorded on single, 3-component (3C), digital receivers. In this way another 3D P-wave as well as a 3D S-wave dataset were acquired. In the active shear-wave experiment, the SHOVER technique (Edelmann 1981) was applied to directly excite shear waves using standard vertical vibrators.

2. STRUCTURAL ANALYSIS

We analysed 7 stratigraphic horizons in detail: Top Aquitanian (1), Top Chattian (2), Top Rupelian (3), Top Priabonian (4), Top Purbeck (5), Basis Reservoir (6) und Top Dogger (7) in a mixed manual and automated picking procedure (Fig. 3). Since the fault morphology was crucial for a later kinematic restoration, we picked faults on random lines perpendicular to the strike of the faults every 50 m.

The survey area is characterized mainly by normal faulting. The largest of these faults is the Munich fault, a prolongation of the known Markt-Schwabener Verwurf, showing a maximum throw up to 350 m. To the east, this fault splits into several branches and terminates. In the SE part of the area, we find another complex fault system that constitute the continuation of faults known from the Unterhaching 3D-seismic. Notably relay-ramps, hook structures and horst and

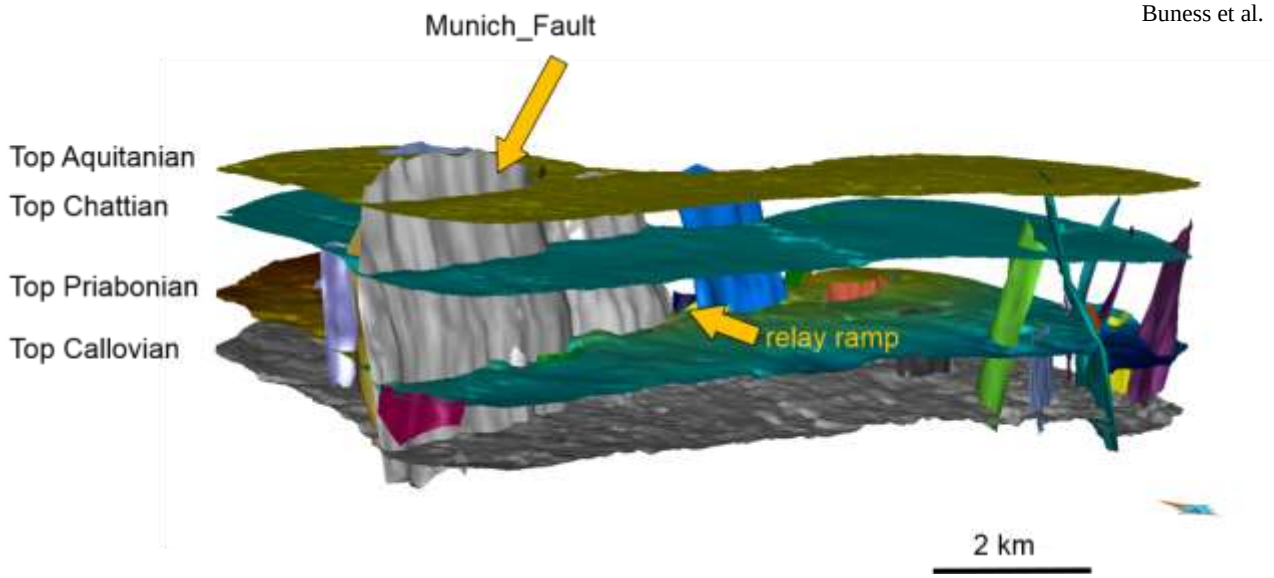

Figure 3: 3D geological model developed from the 3D survey showing four of seven stratigraphic horizons and all faults, 2x vertical exaggeration.

graben structures can be seen. In both parts, small antithetic and synthetic faults with very small throws (<80 m) form part of a horsetail splay, typical for strike-slip regimes (Kim et al. 2004).

Regarding the fault geometry, two characteristics can be observed: firstly, there is a significant steepening of the fault dip when passing from the Molasse sediments into the more competent carbonates. Dip angles range from 60-70° in the molasses sediments to 75-90° in the carbonates. Secondly, the hanging-wall sediments show rollover structures, which are partly brittle, and drag-folds. 2D kinematic modelling shows that these structures result from the varying fault geometry.

Juxtaposition maps (i.e. fault throw vs. strike) allow information on the timing of the faulting to be extracted. They show the maximum throw was during Cretaceous times, i.e. between Top Purbeck and Top Priabonian. Because Cretaceous units are thin and disappear towards the NW, they do not give more detail about the timing of the event. However, fault throw decreases upwards the younger Molasse units as well as downwards to deeper layers at base Malm und Dogger. This indicates that the faults probably do not extend in to the basement, which may be crucial for the interpretation of induced seismicity.

The fault throw along strike at the Top Purbeck level differs that at the Top Priabonian. This implies an erosional phase between these two stratigraphical markers. The geometry of the tiplines gives a hint to the kinematic of faults (Ziesch et al. 2017): pure normal faulting leads to elliptical tiplines. However the vertical trend of some tiplines in the survey area indicate a mixture of normal and strike slip faulting that is confirmed by interpretation of the seismic data.

3. FACIES CLASSIFICATION

Knowledge of facies of the carbonate platform was derived from outcropping units of the Frankonian and Swabian Alp in the north (Fig. 1) and a few boreholes inside the Molasse basin. The traditional model (Meyer and Schmidt-Kaler 1989) includes a distribution of large reef complexes separated by troughs consisting of differently-layered limestones. Whereas in the north coral reefs occur, they could not be confirmed by deep boreholes in the southern part. The distribution and size of these troughs in the Munich region would seem to be highly irregular (Schulz and Thomas 2012).

For seismic facies analysis, we followed an approach that is primarily oriented on the seismic data: The Malm units were divided vertically into 8 layers, each of which with an approximate thickness of 70 m. Inside every layer and for every bin the following three seismic attributes were calculated: (1) centre frequency, (2) amplitude und (3) similarity. The range of centre frequencies and amplitudes were divided into three intervals and the similarity into two intervals. An inspection of the results yielded a strong correlation between amplitudes and similarity values, i.e. small amplitudes show less similarity and vice versa. In this case, we designed a further division of amplitude values according to similarity. This lead to altogether 18 independent combinations (Fig. 4), that we subsequently colour coded and projected on top of each layer.

The distribution of classes reveals regions with uniform amplitudes contrasting with strong variations (s. Fig. 4). These regions can be further subdivided by different frequencies; especially regions with low amplitude values show strongly varying frequencies. The pattern can be correlated between the vertical layers, towards the upper layers amplitudes as well as amplitude differences increase. We furthermore took the local distribution in each layer to interpret sedimentation environments.

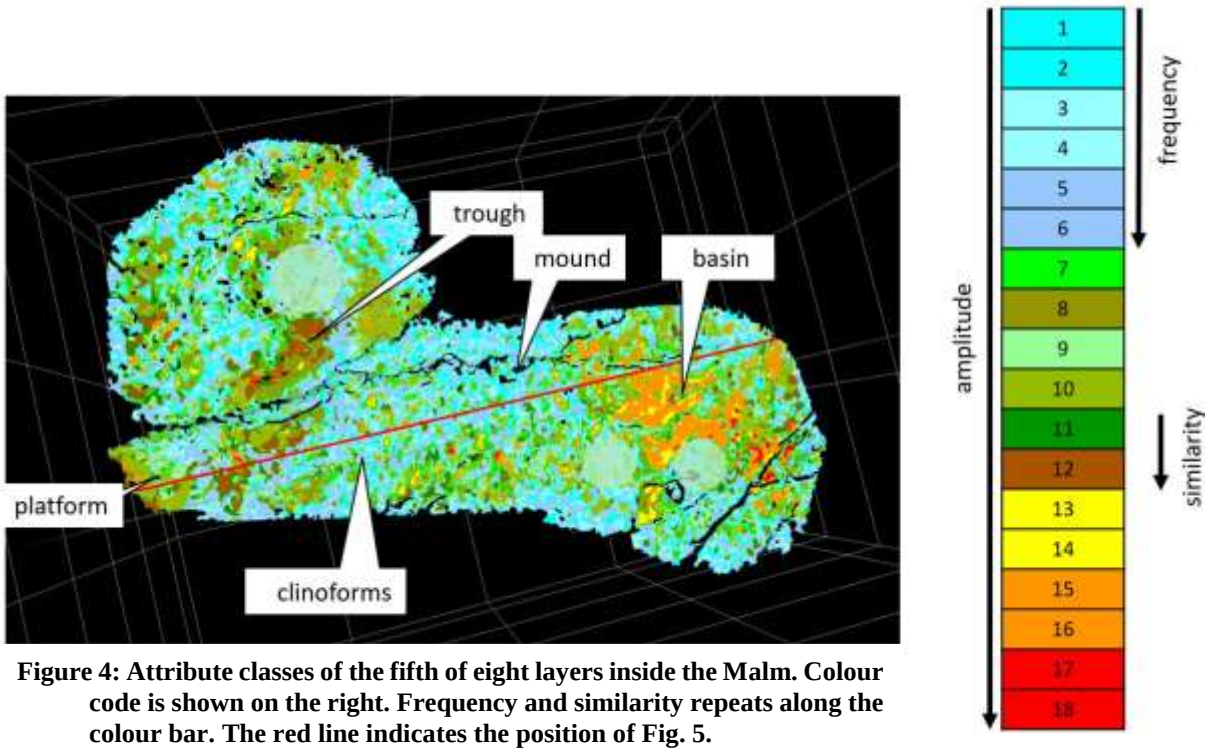

Figure 4: Attribute classes of the fifth of eight layers inside the Malm. Colour code is shown on the right. Frequency and similarity repeats along the colour bar. The red line indicates the position of Fig. 5.

4. SEQUENCE ANALYSIS

To carry out an sequence analysis, we first scanned the data for the typical reflection pattern and tried to correlate single strong horizons across the survey area. The seismic patterns often appear in groups and may be locally confined, but cover larger areas as well. Locally-confined patterns are clinoforms and small triangular structures with upwards pointing tip. Pattern covering larger areas are parallel reflections, sigmoidal and dome-shaped forms. The distribution of these pattern is irregular, i.e. they are not visible in all sections. The correlation of horizons is non-unique, since the reflection characteristics change over the survey area: whereas the eastern and western part shows strongly correlatable horizons, the center part does not, hindering correlation over the whole area. However, four horizons could be found that divide vertically the Malm (Fig. 5). Laterally, clinoforms are confined by seismic transparent as well as seismic chaotic regions. Triangle structures show up next to finely-laminated reflectors and with chaotic patterns inside. A sigmoidal structure appears in the upper half of the Malm, next to chaotic reflectivity. Dome-shaped structures are found in the upper part of the Malm as well, but only in the SE of the survey area.

The classification shown in Figure 4 represents a depth slice approximately at the top of the second layer in Figure 5 and can be thus interpreted: The low reflective

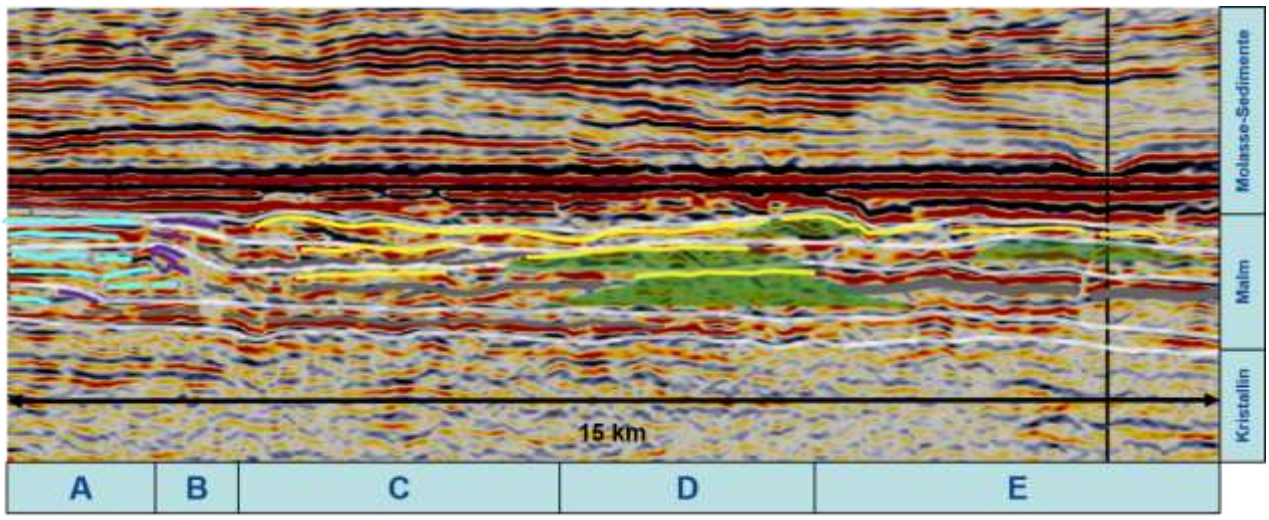

Figure 5: Facies interpretation along the section marked in fig. 4. Shown are sequence boundaries (white), mud-mounds (green), platform mud wackestones (light blue), basin mudstones (grey), shallow water grainstones (yellow) and shelf margin boundstones (purple).

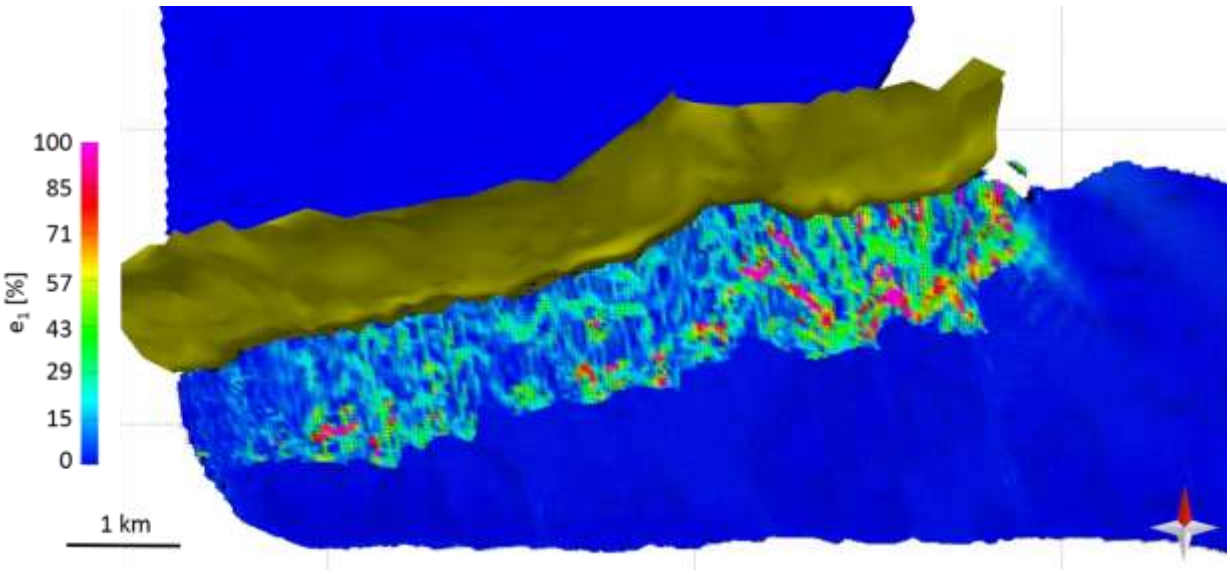

Fig. 6: Deformation at Top Purbeck after 3D retro-deformation of all stratigraphic layers above. Shown is the e1-magnitude, which gives a scalar quantity of the deformation of the hanging-wall. The strongest deformation is found at more than 1 km away from the fault.

region at the eastern margin corresponds to mud mounds that become apparent at the rightmost position in the section. Towards the west, a basin with very high reflectivity follows, which is cut by the section on its northern margin. Further west, a region dominated by mud mounds, characterized by lower reflectivity follows, before small to medium amplitudes indicate a region were clinoforms appear. Further to the west, a trough can be correlated with medium amplitudes. The westernmost region consists of a platform showing little reflectivity. Generally, mud mounds are characterized by circular, low reflectivity structures surrounded by stronger reflectivity and by varying frequencies.

4. RETRODEFORMATION

In a first step, we cut all stratigraphic horizons into single blocks, so they could be moved independently along the fault surfaces. We calculated dip, azimuth, curvature, and cylindricity for all fault surfaces. Altogether, we created 40 blocks consisting of tetrahedra with edge lengths of 75 m.

The second step consists of an assignment of lithology and age of the stratigraphic layers to the volumes. An exact estimation of compaction is crucial for retro--deformation and needs data for porosity. From several databases we calculated exponential porosity-depth functions for all Molasse sediments. Due to the lack of data, the carbonates were modelled using a constant porosity function. Resulting strain values due to decompaction range between 5 % at top Aquitanian to nearly 50 % for the lower Molasse layers. They show no significant lateral variations, only near to the main faults do they decrease.

The next step comprised the retro-deformation of the hanging-wall of the largest fault, the E-W striking Munich fault with a throw of 350 m. Surprisingly, the largest values of deformation (e1-magnitude) do not appear closest to the fault, but 500 – 1000 m south of it. We can also differentiate the deformation laterally: in the western part, it is in mostly small with values that do not exceed 20 %, whereas in the eastern part often values of up to 85% occur. Since deformation is a proxy to the density of sub-seismic fractures, an increased amount of fractures is more probable in the eastern part, close to where the Munich fault splits into two branches. Besides the scalar value of the e1-magnitude, the deformation vectors can be derived from retro-deformation. They give the direction of maximum deformation and thus of the preferred fracture orientation. They are predominantly perpendicular to the Munich Fault. Thus we hypothesize that the Munich fault has a preferentially fault-parallel anisotropic permeability.

4. SHEAR WAVES

Shots in the eastern part of the seismic survey were recorded additionally by 3C receivers arranged on 2D lines (s. Fig. 1). After rotation of components into a radial-transversal coordinate system, we discovered that the most prominent reflections originate from the top of the carbonate platform and that the travel time relationship of the vertical to the radial component is 1.55. This would indicate a rather low VP/VS relationship. However, a 3C vertical seismic profile (VSP) from a nearby well shows a Vp/Vs relationship of more than 2 down to the carbonate platform and thus proves that the main energy recorded by the horizontal components results from converted waves.

Knowing the Vp/Vs relationship allows a converted wave processing of the relative small 3C seismic volume. We could follow continuous horizons in this volume, from the top the reservoir as well as from inside the reservoir and correlated them with reflectors from the P-wave seismic volume. The traveltimes of the corresponding reflectors could now be determined,

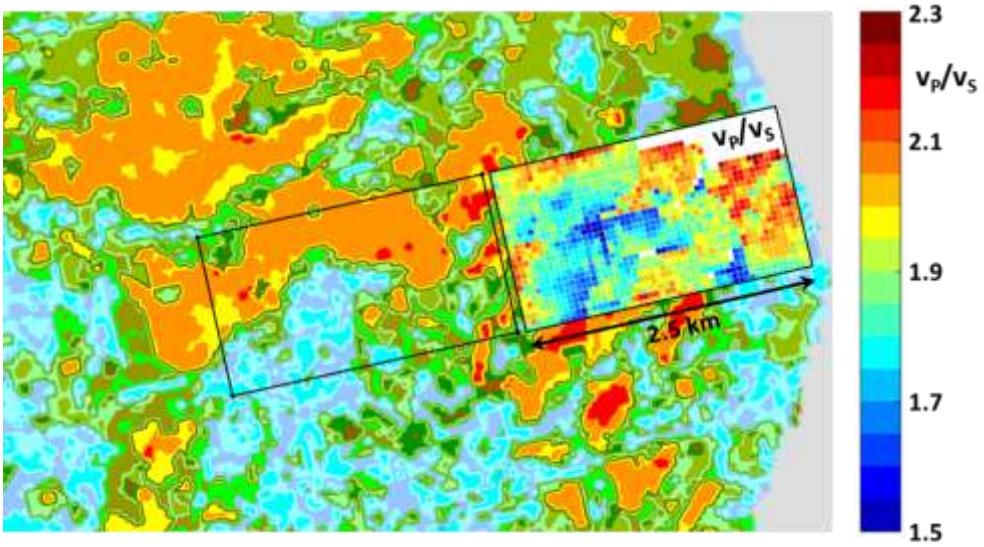

Fig. 7: Vp/Vs relationship observed from interval velocities inside the reservoir inserted in the facies classification map of Figure 4. The pattern of both independently-derived quantities correlate well.

followed by the calculation of the interval travel times between two horizons. This finally gives the Vp/Vs (Garotta 1987, Tessmer and Behle 1988).

The results show a Vp/Vs relationship with a median value of 1.92 above the carbonate platform. This is significantly higher than the values assumed so far (1.6 – 1.7; Schulz and Thomas 2012). This finding is of significance for the determination of hypocentres of induced seismicity occurring at geothermal facilities in the surrounding area (Megies and Wassermann, 2014). The high V_P/V_S relationship hints at events at the basis of the carbonate platform and not deep inside the crystalline basement.

In the reservoir, the variation of the V_P/V_S values from 1.5 – 2.1 is larger than in the Molasse units. In Figure 7, a region of low values (1.5 – 1-8) is surrounded by high values (>1.8). This pattern is opposed to the facies classification (s. Fig. 4). Correlation is possible: low V_P/V_S values correspond to blue facies classes and high values to orange classes. Since the colour code is dominated by the seismic amplitudes, we see low V_P/V_S values where reflectivity is also low and vice versa.

The Vp/Vs relationship allows conclusions to be made about the lithology, facies and porosity that cannot be drawn from either Vp or Vs alone (Tatham & McCormack, 1991). The relationship allows to differentiate between sandstone (1.59-1.76), dolomite (1.78-1.84) and limestone (1.84-1.99) (Domenico 1984). The relationship varies also for different facies: in a lagoon environment lower values than in high porosity limestones have been found by Garotta (1985). Emery & Stewart (2006) show Vp/Vs increases with increasing porosity.

The Vp/Vs relationship correlates in the carbonate platform with Vp and Vs values: high velocities are connected with a low Vp/Vs relationship and vice versa. This can be correlated to the elastic properties of limestone and dolomite. The velocities in dolomite are higher than in limestone, whereas the Vp/Vs relationship is lower (Pickett 1963). The combination of an increase in Vp and Vs correlated with a decrease in the relationship is therefore interpreted as a dolomitized region.

5. THERMAL-HYDRAULIC MODELLING

The basis for thermal-hydraulic (TH) modelling was the structural geological and the reservoir classification, as described above. However, both of them are too detailed to be used directly in a TH-modelling. A consistent reservoir architecture has to be considered for the 3D finite element (FE) net. A modelling of all geological faults is not possible, therefore we build a hierarchy of faults according to the criteria (1) faults that confine the reservoir (2) faults that separate compartments inside the reservoir (3) faults that probably influence the movement of fluid and (4) faults that could act as barriers.

In order to construct a water-tight reservoir-model that is suited for dynamic simulations, we developed the following workflow: smoothing of complex surfaces, homogenisation of triangulated surfaces, removal of gaps, connection of horizon and fault surfaces and association of nodes in the cutting lines between faults and between faults and horizons. In this way, we constructed a geological-consistent, structural- and stratigraphic-unified reservoir model.

Another important aspect constitutes the near- and far-field pressure distribution that result from the constant injection and production of fluids in such geothermal doublet and triplet arrays as well as other multi-well systems such as hexagon patterns. Figure 8 show the pressure field (hydraulic head) after 50 years modelling time caused by a geothermal doublet array and hexagon multi-well systems, respectively.

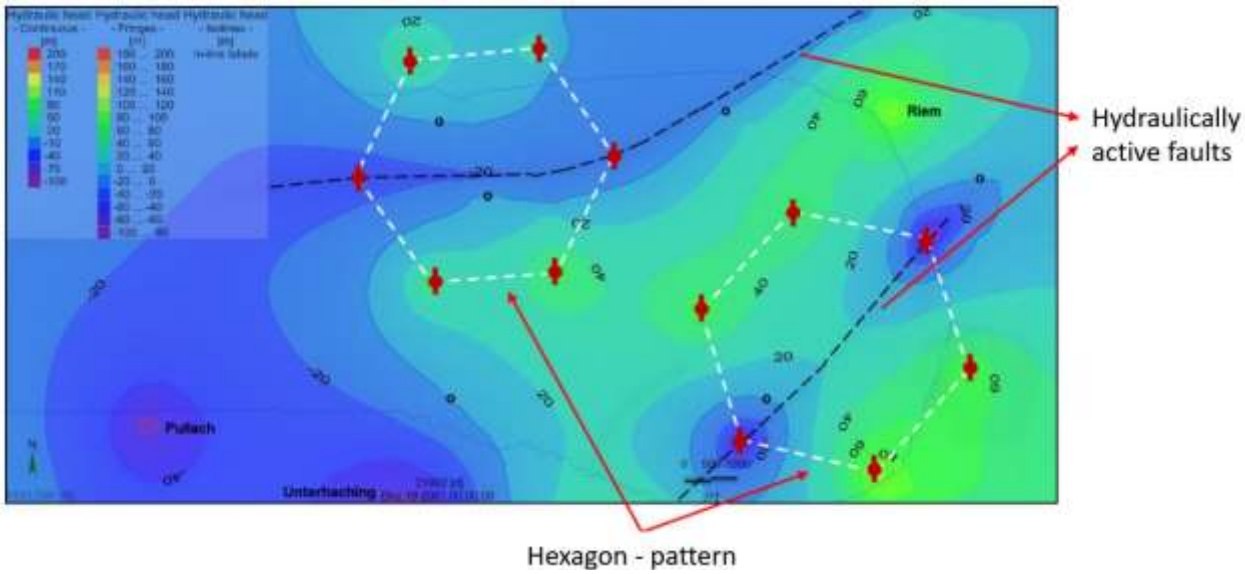

Figure 8: Pressure field (hydraulic head) in the first main influx zone for multi-well configurations (hexagon-configuration of 6 geothermal wells) after 50 years simulation time. Red symbols display injection and production wells. Different hydraulically active faults are shown with black dashed lines. Note that production wells are placed in the fault zones while injection wells are placed around the faults. 150 l/s of thermal water are constantly produced in each production well and 75 l/s of cooled thermal water is permanently reinjected in the injection wells.

A successful optimization of multi-well patterns in highly heterogeneous carbonate reservoirs not only depends on a fine characterization of the reservoir, but also on the complex, long-term, thermal-hydraulic interactions of the multi-well array with existing neighbouring geothermal wells already in operation. Moreover, the well spacing density plays a major role in the generated pressure farfield. Model results indicate that fluid flow regime in the entire region of greater Munich is highly controlled by such high densely-spaced doublet array. A stationary flow regime is established a couple of years after the onset of injection and production. Site-specific thermal and hydrogeological conditions make special multi-well design systems more appropriate than regular geothermal doublet arrays (Fig. 8).

6. CONCLUSIONS

In this project, we have applied methods that have never been used before in the geothermal exploration of the Bavarian Molasse, with promising results. We believe that the combination of seismic sequence stratigraphy and classification algorithms based on seismic attributes leads to a better understanding of the development of the carbonate platform.

The database consisted of a large 170 km2 seismic dataset without well control. Our aim was to understand the overall picture, in this case, the development of the carbonate platform and its overburden. This is impractical if the seismic volume is too small, as it is often the case of geothermal surveys that cover only the immediate surrounding area of a doublet. Although as in our case the survey was quite large, it was able to allow a limited insight into the carbonate depositional processes. In a follow-up project, we will try to expand the seismic database.

The evaluation of multicomponent seismic recording hints at dolomitized regions inside the reservoir. Since the pattern of this distribution correlates with the independently-derived facies classification, we are confident about its reliability. Therefore, we believe it is sensible to conduct future 3C seismic surveys using 3C receivers. During the Munich survey, we compared 3C single sensors with traditional geophone group recordings and did not notice significant differences, despite the noisy urban environment (Wawerzinek et al. 2017).

The technique of retro-deformation enables the prediction of sub-seismic faults (Ziesch et al. 2019). This technique strongly depends on the morphology of fault zones – hence it is crucial to invest enough effort in a detailed fault plane determination. Moreover, we were able to explain by retro-deformation some features in the structure of the Molasse sediments (i.e. rollover and drag folds), which are due to the strong variation of the fault dip above and within the carbonate platform. The prediction of sub-seismic fractures by retro-deformation looks plausible, but needs control by drilling (and FMI data) when the SWM project proceeds.

We included all the findings into a reservoir model and conducted long-time thermal-hydraulic modelling. The transformation of the structural and the facies models needs inevitable simplification before it is applied in such a model. Since new data will come in continuously during future exploitation, rapid updating of the reservoir model is crucial. From our modelling of the status quo knowledge, we conclude, that a multi-well design,

e.g. hexagon configurations, taking site-specific conditions (e.g. faults or facies variation) into account, has significant advantages over a regular array of doublets.

REFERENCES

Buness, H., von Hartmann, H., Lueschen, E., Meneses Rioseco, E., Wawerzinek, B., Ziesch, J. & Thomas, R. (2016): GeoParaMoL: Eine Integration verschiedener Methoden zur Reduzierung des Fündigkeitsrisikos in der bayrischen Molasse, Geothermische Energie, 85, 22-23.

Edelmann, H.A.K. (1981): SHOVER shear-wave generation by vibration orthogonal to the polarization. Geophysical Prospecting 29, 541-549.

Fritzer, T., Settles, E. and Dorsch, K. (2004): Bayerischer Geothermieatlas 2004. Bayerisches Staatsminsterium für Wirschaft, Energie und Technologie, München.

Garotta, R. (1985): Observation of shear waves and correlation with P events. In G. Dohr (ed.): Seismic Shear Waves, Part B: Applications, Geophysical Press.

Garotta, R. (1987): Two component acquisition as a routine procedure. In S.H. Danbom & Domenico, S.N. (eds.): Shear Wave Exploration, Geophysical Developments Series No. 1, Society of Exploration Geophysicists.

Hecht, C. and Pletl, C.(2015): Das Verbundprojekt GRAME – Wegweiser für eine geothermische Wärmeversorgung urbaner Ballungsräume. Geothermische Energie, Heft 82, 2015/2.

Kim, Y.-S., Peacock, D.C.P. & Sanderson, D.J. (2004): Fault damage zones. Journal of Structural Geology, 26, 503-517.

Megies, T. and Wassermann, J. (2014): Microseismicity observed at a non-pressure-stimulated geothermal power plant. Geothermics 52, 36-49.

Meyer, R.K.F., Schmidt-Kaler H., 1989. Paläogeographischer Atlas des süddeutschen Oberjura (Malm), Geologisches Jahrbuch, Reihe A, Heft 115, Schweitzerbart‘sche Verlagsbuchhandlung, Stuttgart.

Pickett, G. R. (1963): Acoustic characterlogs and their application in formation evaluation. Journal of Petroleum Technology 15, 659-667.

Schulz, R. and Thomas, R. (2012): Geothermische Charakterisierung von karstig-klüftigen Aquiferen im Großraum München – Endbericht. LIAG Bericht, Archiv Nr. 130392, Hannover.

Tessmer, G. and Behle, A. (1988): Common reflection point data-stacking technique for converted waves. Geophysical Prospecting 36, 671-688.

Wawerzinek, B., Buness, H. & Thomas, R. (2017): Beschleunigungssensoren bei einer 3D-Seismik in München: Eine Alternative? - Tagung der Deutschen Geophysikalischen Gesellschaft, 27.-30.03.2017; Potsdam.

Ziesch, J., Aruffo, C.M., Tanner, D.C., Beilecke, T., Dance, T., Henk, A., Weber, B., Tenthorey, E., Lippmann, A. & Krawczyk, C.M. (2017): Geological structure and kinematics of normal faults in the Otway Basin, Australia, based on quantitative analysis of 3-D seismic reflection data. Basin Research, 29: 129–148. doi:10.1111/bre.12146.

Ziesch, J., Tanner, D., Krawczyk, C. (2019): Subseismic pathway prediction by three-dimensional structural restoration and strain analysis based on seismic interpretation. AAPG Bulletin, in press (nn 2019), pp. 1–27.

Acknowledgements

We thank Stadtwerke München (SWM) for a good cooperation. The project is supported financially by the Federal Ministry for Economic Affairs and Energy (FKZ 0325787B).